Desalination 520 (2021) 115378

Contents lists available at ScienceDirect

Desalination

journal homepage: www.elsevier.com/locate/desal

# An integrated membrane distillation, photocatalysis and polyelectrolyte-enhanced ultrafiltration process for arsenic remediation at point-of-use

Sergio Santoro [a], Paola Timpano [a], Ahmet Halil Avci [a], Pietro Argurio [a,*], Francesco Chidichimo [a], Michele De Biase [a], Salvatore Straface [a], Efrem Curcio [a,b]

[a] Department of Environmental Engineering, University of Calabria, Via Pietro Bucci CUBO 44A, 87036 Rende, CS, Italy
[b] Seligenda Membrane Technologies SrL, c/o University of Calabria, Via P. Bucci CUBO 45A, 87036 Rende, CS, Italy

## HIGHLIGHTS

- Arsenic remediation of contaminated water via membrane distillation
- Photocatalytic oxidation of arsenite into arsenate
- Polymer-enhanced ultrafiltration for arsenate removal
- Integrated process for Zero Liquid Discharge and groundwater remediation

## GRAPHICAL ABSTRACT

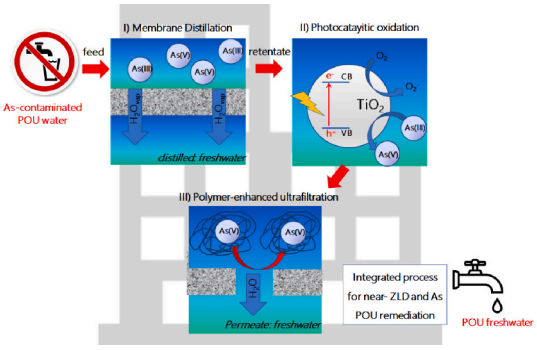


## ARTICLE INFO

*Keywords:*
Arsenic remediation
Membrane distillation
Photocatalysis
Polymer-enhanced ultrafiltration
Zero liquid discharge

## ABSTRACT

Arsenic contamination of drinking water is a result of natural and/or anthropogenic activities, causing undesirable detrimental effects on the environment and the human health. Herein, an integrated process based on Membrane Distillation (MD), photocatalysis and Polymer-enhanced Ultrafiltration (PEUF) was developed for an effective remediation of arsenic (As). This approach, whose effectiveness was demonstrated by experimental tests on artificial solution mimicking As-contaminated water in the area of Sila Massif (Italy), ensured a near total water recovery and a rational management of residual contaminants.

MD allowed to produce high-quality freshwater from contaminated feedwater containing As in the range of 0.059-5 mg·$L^{-1}$, without deterioration of the transmembrane flux up to a recovery factor of 98.8%. Furthermore, a photocatalytic step was applied on MD retentate to convert arsenite As (III) into arsenate As(V), the latter subsequently removed by PEUF with efficiency of 98.2%. Speciation analysis demonstrated the necessity to reduce the feed pH to 5.6 in order to avoid the risk of scaling in MD stage, whereas $Na_2CO_3$ softening at pH 9 before the photocatalytic stage ensured both the reactive precipitation of Ca and Mg ions and the depletion of bicarbonate ions.

* Corresponding author.
*E-mail address:* pietro.argurio@unical.it (P. Argurio).

https://doi.org/10.1016/j.desal.2021.115378
Received 19 July 2021; Received in revised form 24 September 2021; Accepted 26 September 2021
Available online 2 October 2021

## 1. Introduction

The alarming presence of contaminants in water bodies has increased the demand for effective remediation technologies [1–3]. Arsenic (As), highly toxic to humans and classified as a group I carcinogen [4], is a natural component of the earth's crust with an average abundance of 1.7 $mg{\cdot}kg^{-1}$ [5–7]. Thus, As contamination of water is frequently caused by geologic sources since it is contained in more than three hundred minerals such as arsenates (relative abundance of 60%), sulfides and sulfosalts, oxides and arsenites, arsenides, native elements and metal alloys [8,9]. For instance, the presence of As in South America is associated to the volcanism of the Andean orogeny [10]; as a result ca. 14 millions of inhabitants in at least 14 countries are exposed to As contaminated freshwater causing mortality from cancer, cardiovascular and respiratory diseases. [11–13]. The As contamination has been observed especially in proximity of mining sites where the anthropologic activities accelerate its mobility and geochemical cycle [14–16]. In fact, reductive dissolution of iron and aluminum oxides and metal reducing bacteria are widely recognized as the major natural cause of As release from bearing minerals [17], whereas mining, ore processing and metals extraction are the most impacting anthropogenic sources of As in groundwater together with coal burning, As-based wood preservatives (e.g. chromated copper arsenate) and arsenical pesticides [18,19].

Effective technologies for the remediation of As pollution in the water bodies, such as coagulation-flocculation [20], adsorption [21], ion-exchange [22] and oxidation [23] are crucial to reduce the health risk arising from the direct consumption of As contaminated drinking water and water-food nexus. However, sustainable arsenic remediation at full-scale water treatment plants is hindered by both technical and economic issues: abovementioned technologies present critical pitfalls such as expensive and elaborate pre-treatment stages [24], chemical regeneration of the adsorbent materials or ion-exchange reactions [21] and formation of by-products as dangerous sludges in coagulation-flocculation processes [25].

In recent years, membrane processes have experienced increasing success in water treatment [26–29] and their intrinsic modularity for flexible applications, operational simplicity, compactness, minimal foot print and reliability make them suitable also at scale of Point-of-Use (POU) treatments.

In particular, Membrane Distillation (MD) has demonstrated the potential to produce freshwater, theoretically rejecting all non-volatile solutes [30–33], including arsenic [2,34]. Concisely, the MD remediation mechanism is based on the diffusion of low temperature vaporized water (typically in the range of 50-70 °C) through microporous hydrophobic membranes that are able to avoid the penetration of liquid water [35]. While generating high-quality freshwater, MD drastically minimizes the volume of rejected brine, attaining recovery factors up to 90% (seawater) or even greater if operated with low-salinity waters, i.e. significantly higher than those reached by pressure-driven processes (i.e. Reverse Osmosis) [36] and coherently with the concept Zero Liquid Discharge (ZLD) [37–39]. Although MD has not yet reached the commercial breakthrough on a large scale mainly because of its high specific energy consumption with respect to conventional desalination and water treatment technologies, several successful experiences (i.e. Scarab Development AB, TNO Keppel Seghers, Solar Spring Gmbh, Aquastill BV, Memsys, KmX Corporation, Econity, Blue Gold Technologies, i3 Innovative Technologies BV [40]) confirm the commercial availability of MD technology with capacity ranging from 1 to 100 $m^3\ day^{-1}$ for application at the point-of-use (POU). The integration of renewable energy (e.g. solar thermal power) or waste heat is an interesting opportunity to drastically reduce the economic/energetic impact of heating the feedwater, while the energy input required to cool the distillate can be efficiently minimized by adoption of technical solutions such as Air Gap configuration - to limit the conductive heat flux across the membrane - or Permeate Gap configuration - a variant of the Direct Contact MD where raw feed is used as cooling fluid for the distillate.

Definitively, the advantages of MD in arsenic remediation are: (i) insensitivity of the process performance to the composition of the contaminated water (i.e. presence of a wide variety of solutes, pH, oxidation state and concentration of As); (ii) opportunity to design MD systems powered by renewable energy or waste heat [41–43]; (iii) easy integration with other membrane unit operations.

Downstream MD, a robust and feasible decontamination approach named polymer-enhanced ultrafiltration (PEUF), based on the complexation of As with chelating polymer and the subsequent removal of the metal-polymer complex via ultrafiltration (UF), was adopted to achieve a near complete As removal in the highly concentrated low-volume MD retentate [3,44,45]. Arsenic ions naturally occurs in pentavalent (As (V), arsenate) and trivalent (As (III), arsenite) forms, the latter being characterized by lower reactivity and higher toxicity and mobility [46]. PEUF results efficient in removing As(V) from aqueous media, but it is ineffective for the removal of As(III). This behavior can be explained considering the $pK_a$ values of $H_3AsO_4$ ($pK_{a1} = 2.22$, $pK_{a2} = 6.98$ and $pK_{a3} = 11.53$) and the $pK_a$ values of $H_3AsO_3$ ($pK_{a1} = 9.2$, $pK_{a2} = 12.1$ and $pK_{a3} = 12.7$), which are the inorganic forms of As(V) and As (III), respectively. On these bases, at pH below 9.2 the arsenite is uncharged and unable to interact with the complexing polymeric agents, while As(V) is completely dissociated in the ionic forms $H_2AsO_4^-$ and $H_2AsO_4^{2-}$, which can be complexed by the polymer. Thus, As(III) oxidation into As(V) is needed as preliminary step to obtain an effective As removal by PEUF enabling to bind As(V) ions with the polymeric agent via electrostatic attractions. In this respect, photocatalytic oxidation of As(III) to As(V) mitigates its harmfulness, being also accepted as a green process through the exploitation of the solar radiation as energy vector [44]. $TiO_2$ efficiently assists oxidation process thanks to the strong oxidation potential of the photogenerated valence band (VB) holes yielding •OH from the oxidation of surface adsorbed $H_2O$ or $OH^-$ groups [47], whereas oxygen plays the key role of hole-electron scavenger [48]. At the last stage, the removal of macromolecular As-complexes is conducted by conventional UF processes [49,50], where the polymer and its metal-complexes are retained by the membrane, while the non-complexed species permeate through the membrane.

In this work we propose an innovative process for As remediation (Fig. 1) based on the integration of: i) MD in direct contact configuration to ensure freshwater production at 98.8% recovery factor (estimated as the volumetric ratio of the permeate with respect to the initial feed); ii) photocatalysis of the highly concentrated MD retentate to effectively convert arsenite into arsenate; iii) PEUF for the effective removal of arsenate. Remediation process is carried out on an artificial solution mimicking a real contaminated water in the area of Sila Massif in Italy [51]; from a geological point of view, the Sila Mountain consists of Hercynian granite rocks intruded into metamorphites rich of sulphides [52], the latter responsible of water contamination being an As-bearing mineral [53].

A systematic study is focused on the evaluation of the performance of MD process with specific focus on hydrodynamic conditions, on the kinetics of the oxidation of As(III), and on the role of the feed pressure on PEUF effectiveness. Speciation analysis is carried out in order to assess the necessity to acidify feedwater to avoid scaling in MD stage, and to design soda ash softening procedure before the photocatalytic membrane reactor with the aim to promote the reactive precipitation of Ca and Mg ions in the form of dolomite $CaMg(CO_3)_2$.

The proposed process, enabling the production of purified water at high recovery factor and shifting the arsenic decontamination issue from large-volume feedwater to low-volume MD retentate, is potentially implementable as POU of domestic/residential system.

## 2. Materials and methods

### 2.1. Contaminated feedwater

A real As-contaminated water sample from the area of Sila Massif (Italy), whose composition is reported in Table 1, was mimicked by an artificial multi-ion solution prepared by dissolving appropriate amount of $NaHCO_3$, $KHCO_3$, $NaNO_3$, $MgSO_4{\cdot}7H_2O$, $MgCl_2{\cdot}6H_2O$, $CaCl_2{\cdot}2H_2O$, $Ca(OH)_2$, $NaAsO_2$ and $Na_2HAsO_4{\cdot}7H_2O$, all purchased from Sigma-Aldrich (Italy) with purity ≥98%, in ultrapure Milli-Q water.

The ionic composition of all solutions involved in the experimental campaign was determined by high-resolution continuum source atomic absorption spectrometry (HR-CS AAS); nitric acid ($HNO_3$, 65% wt. solution in water) from Carlo Erba Reagenti (Italy) was used to prepare the sample for analyses. In addition, the concentration of arsenite [As(III)] and arsenate [As(V)] ions was measured separately by analytical kits MQuant (Merck, Italy) operating in the ranges 0.005-0.5 $mg{\cdot}L^{-1}$ and 0.02-3.0 $mg{\cdot}L^{-1}$, respectively; results on total As were comparable to those obtained from HR-CS AAS (difference < 5%).

According to data in Table 1, the concentration of total As is 2-3 order of magnitude lower with respect to major cations (e.g., $Na^+$, $Ca^{2+}$, $Mg^{2+}$), while bicarbonates represent almost entirely the anionic species with a concentration 10-folds higher with respect to sulfates.

### 2.2. Materials

Each membrane module MD020CP2N (Microdyn-Nadir GmbH, Germany) used in MD tests was composed of 40 microporous polypropylene hollow-fiber membranes with inner diameter of 1.8 mm, length of 0.5 m, pore size of 0.2 μm, porosity of 70%, membrane thickness of 650 μm and a total membrane area of 0.1 $m^2$.

The photocatalyst used for photocatalytic oxidation of As(III) to As(V) was titanium dioxide ($TiO_2$) P25 type purchased by Evonic-Degussa (Germany) and characterized by a specific surface area of 44 $m^2{\cdot}g^{-1}$, a band gap 3.2 eV, a crystallographic phase of ca. 80% anatase and 20% rutile and an isoelectric point at pH = 6.8 [54,55].

The water soluble polymeric complexing agent was poly(diallyl dimethyl ammonium chloride) (polyDADMAC, 20% wt. solution in water, average $M_W$ = 100,000–200,000 $g{\cdot}mol^{-1}$) purchased from Sigma Aldrich (Italy).

Hydrochloric acid (HCl, 37% *w*/w) from Carlo Erba Reagenti (Italy) and sodium hydroxide pellets (NaOH, 97% purity) from Sigma Aldrich (Italy) were used to adjust the pH of the aqueous solutions. A pH meter (WTW Inolab Terminal Level 3) with a glass pH-electrode SenTix 81 (WTW, Germany) was used for pH measurements.

**Table 1**
Ionic composition of As-contaminated water from Sila Massif, Italy (Figoli et al., 2020).

| Ion | Concentration (ppm) |
|---|---|
| $Na^+$ | 21.9 |
| $K^+$ | 1.8 |
| $Ca^{2+}$ | 12.5 |
| $Mg^{2+}$ | 7.3 |
| $Cl^-$ | 10.3 |
| $HCO_3^-$ | 117 |
| $NO_3^-$ | 0.6 |
| $SO_4^{2-}$ | 9.3 |
| As | 0.059 [10% as As(III)] |
| pH | 7.8 |

### 2.3. Integrated process for As remediation

#### 2.3.1. Ion speciation

PHREEQC v.3 software with phreeqc.dat database, released by U.S. Geological Survey, was used to predict the thermodynamic behavior of the multi-ion solutions and to simulate conditions for salts precipitation as a function of pH and temperature.

#### 2.3.2. Membrane distillation (MD)

The remediation of As contaminated solution was carried out by a direct contact MD system operated with two modules MD020CP2N arranged in parallel. Both feed (artificial groundwater) and distillate (deionized water) streams were continuously recirculated at the same flowrate by a two-channel peristaltic pump iPump YZ15A (Fluid Technology, China), in countercurrent-flow mode, varying the Reynolds numbers (*Re*) from 47 to 107.

Feed inlet temperature was fixed at 60 °C by a heater Mod. 112A (VWR, Italy), whereas the inlet distillate temperature was kept constant at 20 °C using a Digital Plus Neslab RTE201 thermostatic bath (Thermo Scientific, Italy). The temperatures of the streams were measured at the inlet and the outlet of the membrane modules by Sper Scientific 800,012 Pt multi-channel Type-K thermocouples with sensitivity ±0.1 °C (Cole-Parmer, US). The transmembrane flux was calculated from weight variations (±0.1 g) over time using a balance (Ohaus ScoutPro SP601, OHAUS Europe GmbH, Germany) connected to the distillate tank.

#### 2.3.3. Photocatalysis

Photocatalytic oxidation of arsenite into arsenate was performed in a cylindrical Pyrex glass batch reactor of 500 mL shown in Fig. 2. The MD retentate was charged to the photoreactor and, under magnetic stirring, $TiO_2$ catalysts was added to achieve a concentration of 0.05 $g{\cdot}L^{-1}$, appropriate to photo-oxidize As(III) to As(V) while limiting light

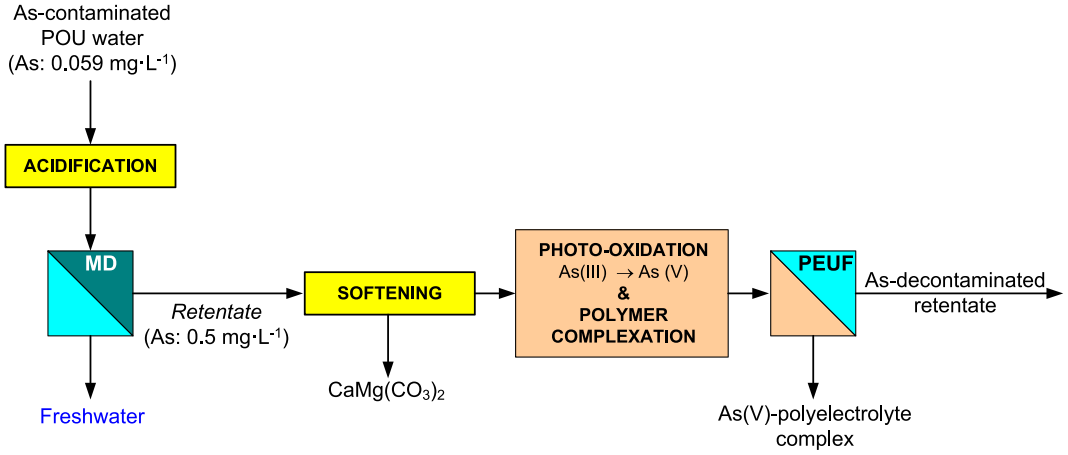


**Fig. 1.** Scheme of the integrated process for As remediation (MD: membrane distillation; PEUF: polymer-enhanced ultrafiltration).

scattering by photocatalyst particles. The operating pH was fixed to 9 considering that: i) the thermodynamic driving force for the photo-oxidation process, i.e. the difference between the redox potential of the As(V)/As(III) couple and the valence band potential (EVB) increase with the pH; ii) the As(III) adsorption and the As(V) desorption are favored at alkaline pHs due to the electrostatic interactions between As (III) or As(V) ions and the photocatalyst surface.

The photocatalytic reactor was equipped with a Hg lamp (Helios Italquartz, Italy) axially positioned emitting in the range from 240 nm to 440 nm (125 W), with a maximum emission peak at 366 nm and a medium light intensity of 0.43 $mW \cdot cm^{-2}$. Thermostatically controlled water recirculated in the pyrex glass jacket by Polystat CC1 (Huber, Germany) allowed to fix the temperature of the photoreactor. Oxygen was bubbled into the photoreactor maintaining a constant concentration of 22 ppm, controlled by means of the portable dissolved oxygen meter HI 9143 (Hanna Instruments, US) equipped with a membrane selective electrode.

A series of photocatalytic tests were carried out by changing the irradiation times (2, 5, 10, 20, 30 and 60 min) in order to evaluate the kinetics of the photocatalytic oxidation of As(III) to As(V).

The solutions collected at the end of each photocatalytic test were submitted to microfiltration by using a polypropylene membrane disc filter GH-Polypro (Pall Corporation, US) with a thickness of 101 μm and 0.2 μm nominal pore size with the aim to remove the photocatalyst before adding the polymer complexing agent.

#### 2.3.4. Polyelectrolyte-enhanced ultrafiltration (PEUF)

Once the MD retentate was treated by photocatalytic oxidation of As (III) to As(V) and the photocatalyst was removed by MF, the complexation of As(V) by the polymeric complexing agent polyDADMAC was carried-out by using the operative conditions determined in [44]. Briefly, polyDADMAC was added the As(V) contaminated solution adjusting the polyelectrolyte/As weight ratio at 30 and the pH at 9 by adding dropwise NaOH solution under vigorous stirring. Several studies demonstrated that water-soluble polymers with quaternary amine groups were effective for removing As(V) [49,50,56]: their removal mechanism is essentially based on the anion exchange between the chloride counterions of quaternary ammonium salt and the As(V) ions [57].

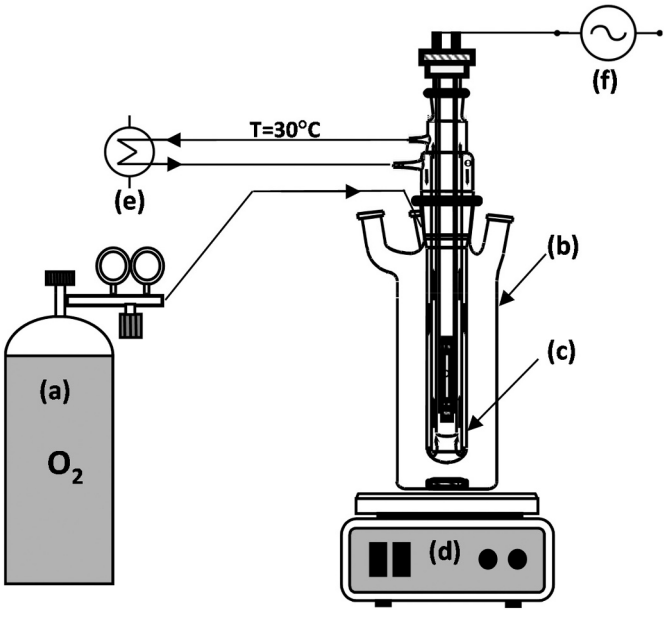


**Fig. 2.** Schematization of the batch photocatalytic reactor: (a) oxygen cylinder, (b) photoreactor, (c) medium pressure Hg lamp with cooling jacket, (d) magnetic stirrer, (e) heat exchanger, (f) power source.

PEUF experiments were carried out using a membrane module A-02910-41 purchased by Cole-Palmer (US) equipped with UF Iris 30 Tech-Sep polyethersulfone (PES) membrane with molecular weight cut-off 30 kDa and active area of 9.6 $cm^2$. Experiments were conducted at room temperature and at relative feed pressure within the interval 1-4 bar.

## 3. Results and discussion

### 3.1. As remediation via acidification and membrane distillation (MD)

MD is a hybrid thermal-membrane process whose driving force to mass transfer in vapor phase is given by a partial pressure gradient established between the opposite sides (retentate and distillate) of a microporous hydrophobic membrane. Unlike Reverse Osmosis and other pressure-driven membrane operations, MD is not limited by osmotic and concentration polarization phenomena; as a result, the poor sensitivity towards the concentration of ions, especially in treating diluted aqueous solutions such as groundwater, allows at reaching high water recovery factors [58]. However, under these circumstances, scaling due to the precipitation of sparingly soluble salts such as $CaCO_3$ and $CaSO_4$ may represent a critical issue [59,60], exacerbated by the thermal nature of the driving force in MD, being the gypsum and calcium carbonate solubilities inverse with temperature [32].

Modelling Ca, Mg and $CO_3^{2-}$ ionic speciation via PHREEQC (Fig. 3.a-c) reveals that the progressive dehydration of As-contaminated groundwater at a natural pH of 7.8 results in the supersaturation for carbonate salts at water recovery factor above 50%.

As expected, the extent of carbonates precipitation is drastically enhanced with the recovery factor: more than the 95% of the solutes are predicted to precipitate at a recovery factor of 98.8%, mostly in form of dolomite $CaMg(CO_3)_2$. Definitively, the precipitation of sparingly soluble salts on the membrane surfaces is a serious limitation that must be properly addressed to avoid a reduction of the efficiency and the stability of MD.

Besides the employment of antiscaling agents [61,62], the acidification of the feed is commonly employed to convert carbonates into bicarbonates modifying the equilibrium in seawater [63] as following:

$$Ca^{2+} + HCO_3^- \leftrightarrows H^+ + CaCO_3 \quad (1)$$

Equilibrium data in Fig. 3 confirmed that a decrease of pH to 5.6 allowed to hit water recovery factor of 98.8% avoiding the precipitation of $Mg^{2+}$, $Ca^{2+}$ and $CO_3^{2-}$ ions in the MD retentate.

We here anticipate the positive impact of acidification in decreasing the concentration of bicarbonate ($HCO_3^-$) ions present in groundwater (Table 1) on the photocatalytic oxidation of As(III) to As(V). It is recognized that bicarbonate ions ($pK_{a1}$ and $pK_{a2}$ for $HCO_3^-/CO_3^{2-}$ system are 6.3 and 10.3, respectively [64]) can compromise the photocatalytic activity, leading to the formation of inorganic radicals upon the interactions with holes and hydroxyl radicals, described by the following reaction:

$$HCO_3^{2-} + OH \dot{\rightarrow} HCO_3^{-\cdot} + OH^-, \quad (2)$$

competing with As onto the photocatalytic surface of $TiO_2$ nanoparticles [65]. Literature studies revealed that the presence of $HCO_3^-$ in groundwater substantially reduced (ca. 52%) the As(V) absorption on $TiO_2$ [66]. Additionally, bicarbonates can represent a serious limitation in the PEUF process because of interactions with the polycationic polymer reducing the active sites available for the chelation of As(V).

According to Fig. 4, acidification reduces the temporary hardness by promoting the conversion of bicarbonates into carbon dioxide [67], i.e. shifting to product side the equilibrium reaction:

$$HCO_3^{2-} + H^+ \leftrightarrows CO_2 + H_2O. \quad (3)$$

Overall, acidification to pH 5.6 reduced by 82% the concentration of

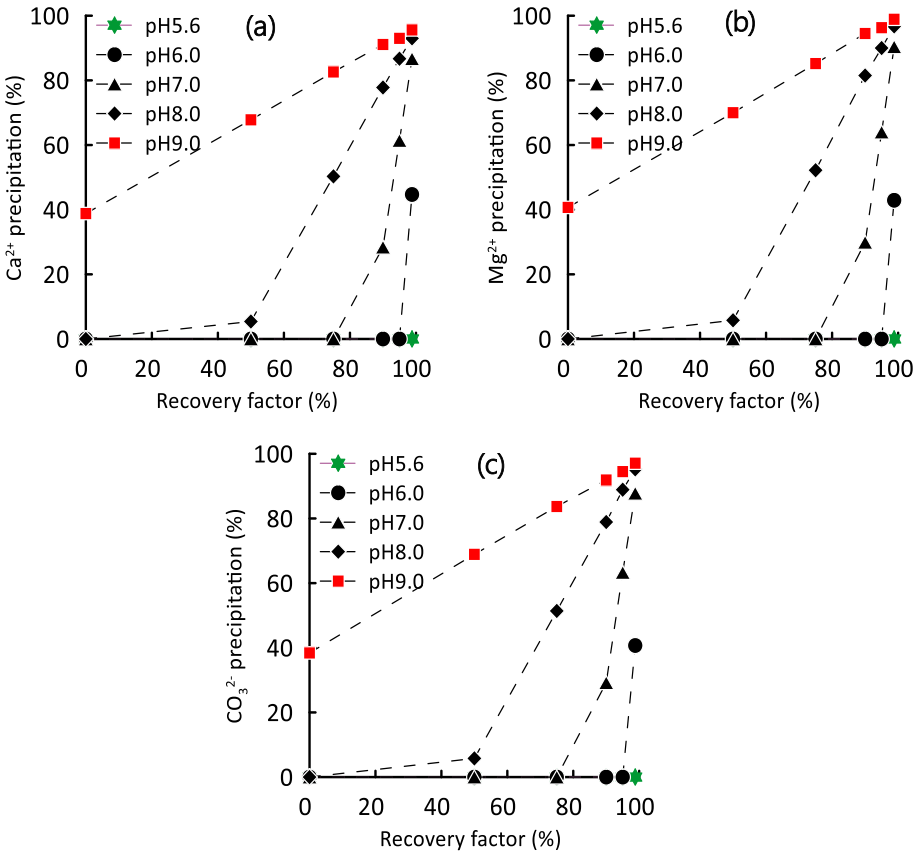


**Fig. 3.** Precipitation of a) calcium, b) magnesium and c) carbonate ions at different pH and recovery factor.

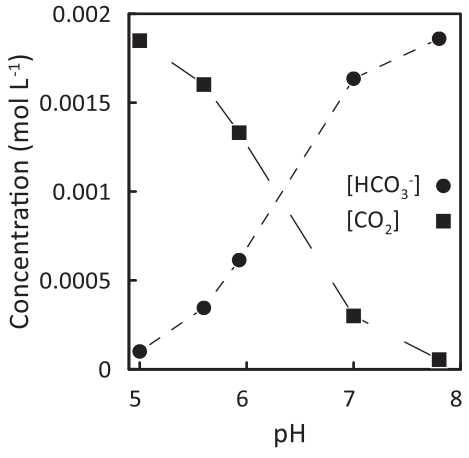


**Fig. 4.** Conversion of $HCO_3^-$ to $CO_2$ versus pH at 60 °C.

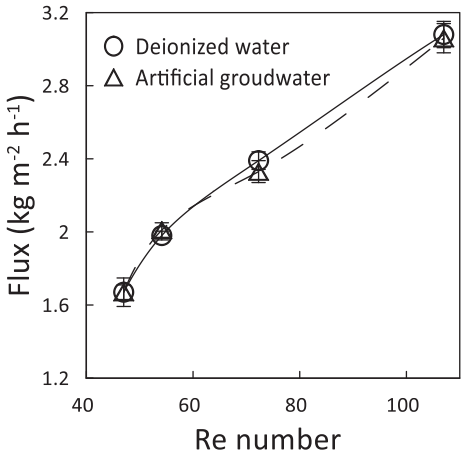


**Fig. 5.** MD flux for pure water and artificial contaminated water (As(III): 0.0059 mg·L$^{-1}$) at different feed flowrates. All tests were conducted at inlet feed temperature of 60 °C and inlet distillate temperature of 20 °C.

bicarbonates within the feed water, i.e. from the initial value of 1.92 mM (from Table 1, with $HCO_3^-$ molecular weight = 61.02 g·mol$^{-1}$) to 0.345 mM.

Average values of the transmembrane flux in MD, fed with either pure water or acidified artificial groundwater, are reported in Fig. 5 as a function of flowrate and at constant feed and distillate inlet temperatures (60 °C and 20 °C, respectively). Experimental observations demonstrated similar evaporation rate under the same operative conditions; this is theoretically supported by the negligible difference in water activity coefficient between de-ionized water and artificial groundwater, as calculated by PHREEQC. At most, when the recovery factor attained 98.8%, the predicted water activity coefficient of the multi-ion solution declined to 0.99, very close to the limit value of 1 characterizing an ideal solution. The increase of feed flowrate and – consequently - of the dimensionless Reynolds number (*Re*), was found to be beneficial to the MD performance. Therefore, a transmembrane flux enhancement by 184% was obtained when *Re* increased from 47 to 107 (1.7 kg·m$^{-2}$·h$^{-1}$ at *Re* = 47; 3.1 kg·m$^{-2}$·h$^{-1}$ at *Re* = 107). Since this effect was more pronounced at low *Re*, the evaporation rate is expected to reach a plateau at higher flowrates.

The improvement of mass transfer consequent to an increase of *Re* is, in part, due the reduction of temperature polarization due to a better

local mixing of the fluid in proximity of the membrane interface [31,68]. In general, the temperature polarization is recognized as a critical issue in MD: heat losses associated to both the latent heat of water evaporation and the thermal conduction through the membrane cause a progressive decrease of the temperature across the boundary layer adjacent to the membrane [69], reducing the effective driving force and worsening the performance of the process [30,31]. Higher *Re* improved the turbulence in the channels of both feed and distillate streams, leading to a reduction of the boundary layer resistance and improving the heat transfer coefficient (h). This was confirmed by calculating h as:

$$h = \frac{Nu \cdot k}{D_h} \tag{4}$$

where k is the water thermal conductivity, $D_h$ the hydraulic diameter of the compartments and *Nu* the Nusselt dimensionless number (i.e. the ratio of the convective to diffusive heat transfer) estimated according to the following empirical correlation under laminar flow:

$$Nu = 3.36 + \frac{0,0036\, RePr \frac{D_h}{l}}{1 + 0,0011\left(RePr \frac{D_h}{l}\right)^{0.8}}; \tag{5}$$

where *Pr* is the Prandlt number and *l* is the characteristic lenght [70–72]. The computed results revealed an improvement in the values of h of the permeate from 3550 $kJ \cdot h^{-1} \cdot m^{-2} \cdot K^{-1}$ to 3600 $kJ \cdot h^{-1} \cdot m^{-2} \cdot K^{-1}$ and of the retentate from 2380 $kJ \cdot h^{-1} \cdot m^{-2} \cdot K^{-1}$ to 2430 $kJ \cdot h^{-1} \cdot m^{-2} \cdot K^{-1}$ when raising *Re* from 47 to 107. The beneficial effect is amplified by the exponential relationship existing between temperature and vapor pressure, as established by Clausius-Clapeyron equation [73].

An additional and relevant contribution to the enhancement of the MD performance when operating with increasing flowrate was provided by the reduction of the residence time of retentate and distillate solutions within the membrane module; this allowed at mitigating the heat exchange between the warm feed and the cold permeate and, hence, at reducing the temperature drop along the axial direction of the module. In fact, the residence time, estimated from the ratio of the dead-volume of the membrane module compartments on the streams flow rates, drastically decreased by 54% (from 0.57 s to 0.26 s in the feed and from 1.27 s to 0.58 s in the distillate) when increasing Re from 47 to 107. Consequent benefits were confirmed by monitoring the outlet temperatures at the shell-and-tube MD module: outlet feed temperature raised from 40.3 ± 0.3 °C to 41.7 ± 0.2 °C, coupled to a declining of the outlet distillate temperature from 32.3 ± 0.2 °C to 30.8 ± 0.3 °C. Definitively, the improvement of *Re* from 47 to 107 led to an enhancement of the driving force as confirmed by the estimation of logarithmic mean temperature difference varying of +1.5 °C, i.e. from 23.8 °C to 25.3 °C [74]. Accordingly, the ultimate result is a gain in the mean value of the water vapor pressure raised from 29.4 mbar to 32.1 mbar with a subsequent improvement of the distilled water. Fig. 6 shows that MD allowed to efficiently treat the contaminated water; the concentration of arsenite, the most recalcitrant As ionic species to membrane filtration operations such as Nanofiltration and Reverse Osmosis, increased in the retentate stream from its initial value of 0.0059 $mg \cdot L^{-1}$ up to 0.5 $mg \cdot L^{-1}$.

Analysis of the distillate (total arsenic concentration below the ICP-MS detection limit of 0.01 $mg \cdot L^{-1}$) confirmed both the good stability of MD (absence of wetting phenomena and complete As rejection) over 8 h c.a of operation and its effectiveness in producing a decontaminated distillate whose quality fits the currently recommended limit for drinking-water fixed by the WHO.

### 3.2. Photo-oxidation of As(III) to As(V) and PEUF

The MD retentate stream, with concentration As(III) of 0.5 $mg \cdot L^{-1}$, was subjected to a photocatalytic oxidation step to turn As(III) into As (V); the latter was then complexed and removed in the final PEUF step. In order to prevent the precipitation of sparingly soluble salts of Ca and

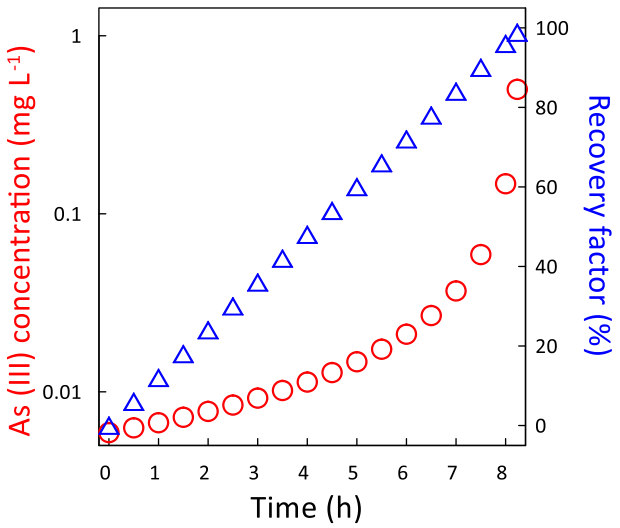


**Fig. 6.** Evolution of the concentration of As(III) in the retentate stream and recovery factor during Direct Contact MD test [Re = 107, inlet feed temperature: 60 °C, inlet distillate temperature: 20 °C].

Mg within the reactor, the retentate was softened by addition of $Na_2CO_3$ at pH 9, overall resulting both in the conversion of residual $HCO_3^-$ into $CO_3^{2-}$ and in the precipitation of dolomite $CaMg(CO_3)_2$, potentially useable for the re-mineralization of the MD distillate [75]. In fact, desalted water usually presents a minimal hardness, and simple strategies of re-mineralization (i.e. direct dosage of a variety of chemicals, blending of the desalination permeate with external water sources or calcite and dolomite dissolution) are necessary to secure its employment in domestic and agricultural uses [76].

After removing hardness, the retentate solution was fed to the photoreactor. The decreasing trend of As(III) concentration in time (Fig. 7.a) was coherent with a first-order kinetic [55]:

$$As(III)_t = As(III)_0 \bullet \exp(-kt) \tag{6}$$

where $[As(III)]_0$ and $[As(III)]_t$ are the concentration of As(III) at the irradiation time $t = 0$ min and at the generic irradiation time t, respectively, and *k* is the observed first-order rate constant. The performance of the photocatalytic process ($R^2 = 0.960$) was adequately predicted by assuming a kinetic constant k of 0.123 $min^{-1}$.

The almost complete conversion of As(III) to As(V) in a 500 mL batch of 83-fold dehydrated MD retentate required a reaction time of 60 min and 0.125 kWh energy. To achieve the same performance, 500 mL of raw water requires a reaction time of 23 min (as per Eq. (6)) and 0.049 kWh energy, that scaled-up linearly to a 83-fold higher volume gives 4.05 kWh. This confirms that the photocatalytic oxidation of As in MD retentate is substantially more feasible than in a large volume of raw water.

Feed solution treated within the photocatalytic reactor was microfiltered to remove the catalyst; then, the permeate - with total As concentration approaching 5 $mg \cdot L^{-1}$, almost completely present in the oxidated As (V) form - was subjected to PEUF stage. Here, the water-soluble poly-DADMAC efficiently bonded arsenate ions producing a polymer–arsenate macromolecules easily rejected by UF membranes thanks to a size-exclusion mechanism; on the other hand, the unbound arsenite remains solubilized into the water and easily permeates through the UF membranes [57].

The evaluation of As (III) concentration into the permeate of the UF step offers the opportunity to estimate the efficiency of the integrated photocatalytic oxidation-PEUF process (η), estimated as:

$$\eta\,(\%) = \frac{As(III)_{R,MD} - As(III)_{P,UF}}{As(III)_{R,MD}} \bullet 100 \tag{7}$$

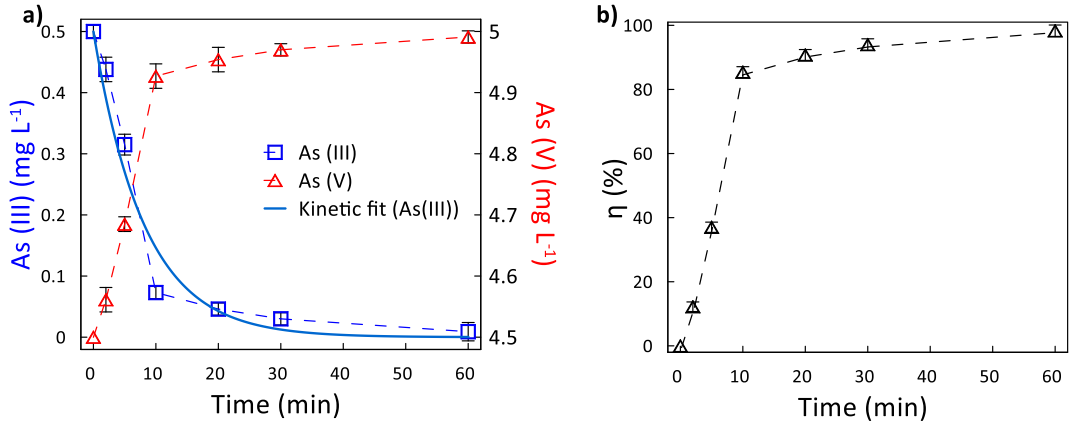


**Fig. 7.** a) As(III) and As(V) concentration as a function of the irradiation time in photocatalytic reactor; b) efficiency of photocatalytic-PEUF process (UF feed pressure: 2 bar).

where $[As(III)]_{R,MD}$ is the initial As(III) concentration in the retentate of MD submitted to photocatalytic reactor and $[As(III)_{P,UF}]$ is the As(III) concentration in the permeate of the PEUF step. As reported in Fig. 7.b, it was noticed that arsenite concentration into the PEUF permeate dropped from 0.5 mg·L$^{-1}$ to 0.009 mg·L$^{-1}$ by extending the irradiation time of the photocatalytic step from 0 to 60 min, with an efficiency of photo-oxidation of 98.2%.

The polymer exchanger is highly reactive towards bivalent ions present at alkaline pH, but the oxidation altered the pH of the medium acting on the protonation of As(V) [77]. Moreover, the values of pKa of As species indicate the significant dependence of charge of the anions from the pH evidencing ultimately the low tendency of As(III) to form anions at neutral pH. Definitively, the ion exchange reaction between the polymer and the As ions is faster at high pH because the bivalent form of As ($HAsO_4^{2-}$) dominates with respect to the monovalent ($H_2AsO_4^-$) [65].

In addition, the polarity of the functional group of polyDADMAC is a crucial parameter governing the selectivity and the retention capacity of ion exchange because its positively charged quaternary ammonium group interacts with the As(V) ions [57]. Thus, these interactions are optimized in alkaline solution because divalent As(V) species are predominant, and, alkaline pH are required to ensure an efficient photo-oxidation and complexation [78].

During this final step, UF was carried out at different relative pressure of the feed in order to evaluate the influence of this parameter on system performance. Results, summarized in Fig. 8, evidenced the benefits of the feed pressure on the permeation rate: the water flux was improved from 112 L·m$^{-2}$·h$^{-1}$ to 334 L·m$^{-2}$·h$^{-1}$ when increasing feed pressure from 1 to 4 bar. Below 2 bar, the results evidenced the linear dependence of flux by the feed relative pressure; under this circumstance, concentration polarization phenomenon was negligible and only the membrane contributed significantly to the mass resistance [79]. On the other hand, the flux deviated from the linear behavior at pressure of 4 bar, and the UF permeability decreased of ca. 15% in comparison with the one observed by feeding pure water. This was essentially related to both concentration polarization, consisting in the accumulation of retained solutes at the membrane surface, and fouling, caused by adsorption and/or deposition of polyelectrolyte on the membrane pores [80–83]. The quality of permeate, expressed in terms of As concentration, did not change significantly with the operating pressure: the average As concentration in the permeate was 100 μg L$^{-1}$, corresponding to As removal of 98.0%. This value is slightly lower than the efficiency of photo-oxidation (98.2%) because of the incomplete complexation of As (V) due to the polydisperse nature of the polymer. Definitively, the integration of photo-oxidation and PEUF as downstream process for MD retentate increased the overall water recovery to 99.97% coherently

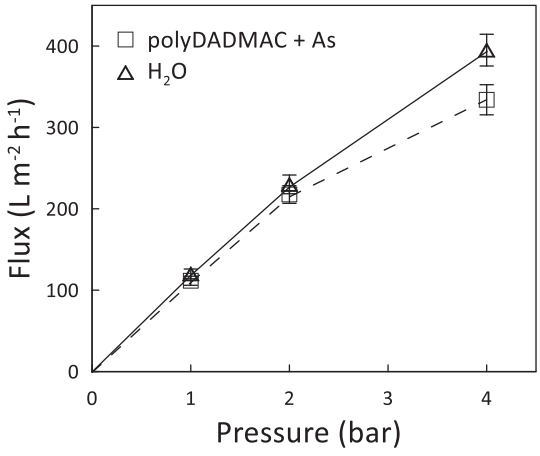


**Fig. 8.** Comparison of the performance of the UF process by feeding pure water and the As-contaminated solution containing polyDADMAC.

with the ZLD approach and mitigated its environmental risk.

From a practical point of view, 1 m$^2$ of membrane is able to remediate via MD ca. 50 L of As contaminated water in 16 h at a rate of 3 3.1 kg·m$^{-2}$·h$^{-1}$, sufficient to reach the minimum per capita water consumption established by WHO [84] at a cost of $6.80·m$^{-3}$ (estimated on a standalone MD set-up solely powered by grid electricity [85]), fairly attractive in rural or arid regions. The post-treatment of the minimal volume of MD retentate has a low energetic and economic impact: 0.25 KWh per liter (<0.1 $) with an estimated capital expense in the range of 1000-2000$. Interestingly, the potential of MD to recovery up to 98.8% of pure water paves the way for the economic viability of advanced oxidation practice, decreasing by 2 order of magnitude the volume (and, roughly, the treatment cost) of the As contaminated waters. Further advantages are related to a radical abatement of the capital cost and footprint in comparison to direct feedwater treatment.

Lastly, UF requires a total capital and operational cost of $0.234·m$^{-3}$ ([85]), which can be doubled by considering the price of the chelating complex and its effect on the shelf-life of the membrane because of fouling. Overall, the purposed process is able to remediate As contaminated water without the production of wastewaters at a cost lower than $10·m$^{-3}$.

The extent of photocatalytic oxidation depends on light sources (UV, visible, and solar), the type of photocatalyst, and experimental conditions (pH, photocatalyst dosage, initial concentration of inorganic ion, light intensity, etc.). Visible-light-active photocatalysts are applied by several researchers to exploit sunlight and to make the photocatalysis

process sustainable. Analogously, energy demand for MD can be efficiently satisfied by converting sunlight into heat by using a solar thermal collector or photothermal materials embodied into the membranes. In the future, the exploitation of the solar radiation in the photocatalysis and MD will make the integrated processes economically more efficient.

## 4. Conclusions

The novel process here discussed, based on the integration of membrane distillation (MD), photocatalysis and polyelectrolyte-enhanced ultrafiltration (PEUF), exhibited interesting performance in the remediation of As-contaminated water.

MD in direct contact configuration, carried out under a moderate temperature gradient (40 °C difference between feed and permeate inlet temperature), was able to produce high-quality freshwater with significant advantages in terms of sustainability (possibility to operate with waste or solar heat) and versatility (modularity for an easy scale-up) with respect to conventional techniques such as coagulation-flocculation, adsorption, ion-exchange and oxidation.

Experiments demonstrated the possibility to dehydrate a multi-ion solution initially containing 0.059 $mg{\cdot}L^{-1}$ of total As (10%*w/v* arsenite) up to a final concentration of c.a 5 $mg{\cdot}L^{-1}$, thus reaching a water recovery factor of 98.8% and obtaining a retentate concentrated 83-folds c.a with respect to the initial solution.

The photocatalytic reactor, fed with the MD retentate, ensured the oxidation of the arsenite into arsenate with efficiency of 98.3%. This step mitigated the toxicity of As and favored its immobilization in poly-DADMAC and its subsequent removal using ultrafiltration (UF) raising the water recovery factor of the integrated process to 99.97%.

A critical assessment of the integrated membrane process revealed the necessity to reduce the pH of artificial feedwater down to 5.6 in order to: i) avoid the of the risk of scaling in high-recovery MD operation; ii) reduce the concentration of bicarbonate ions for a more efficient downstream photocatalysis.

On the other side, softening of the MD retentate at pH 9 was required in order to: i) prevent scaling within the photoreactor; ii) remove coexisting competitive ions by precipitating them as dolomite.

The integrated process can be designed at different scale, from domestic to industrial applications, ensuring the remediation of As-contaminated feedwater and avoiding the production of undesirable wastewater according to the ZLD paradigm. Roughly, a cost of ca. $10 per day are required to produce 1 $m^3$ of freshwater, sufficient for the realization of the right to water of a small community of 20 persons, and the post-treatment of the byproduct making the integrated process of interest for a sustainable point-of-use arsenic remediation.

Although the present experimental activity refers to an Italian case-study, the proposed approach schematized in Fig. 1 is potentially replicable in different geographical scenarios. In Chile, intensive mining activities are a major source of arsenic contamination of groundwater [2]; here, the exploitation of waste heat and solar thermal power (northern regions have an annual direct normal irradiation of approximately 9-10 $kWh{\cdot}m^{-2}$ per day) has the potential to significantly mitigate the cost of MD (about $\$1.6{\cdot}m^{-3}$ when operated with brackish water [85]), making it competitive with Reverse Osmosis. Arsenic contamination is also a severe issue in many Southeast Asian countries such as Pakistan (where a study of Shakoor et al. (2018) revealed that 75% of groundwater wells in five different areas of Punjab exceeded the safe As limit set by WHO [86]) and India (where As contamination involves 20 states and 4 Union Territories [87]). In all cases, the variety of the composition of the contaminated waterbodies imposes tailored conditions of acidification and softening to reduce the risk of scaling in MD and the depletion of competitive ions in the photocatalysis and PEUF.

Nevertheless, the effective implementation of the proposed integrated process, in the same way as most of water decontamination technologies, depends on proper disposal approaches for arsenic-bearing wastes (i.e. As-polymer complex) generated during remediation.

## CRediT authorship contribution statement

**Santoro Sergio:** Conceptualization, Investigation, Data curation, Writing – original draft. **Paola Timpano**: Investigation. **Ahmet Halil Avci:** Formal analysis. **Pietro Argurio:** Conceptualization, Investigation, Writing - Review & Editing, Supervision. **Francesco Chidichimo:** Data Curation. **Michele De Biase:** Visualization. **Salvatore Straface:** Supervision, Project administration. **Efrem Curcio:** Conceptualization, Data curation, Writing – original draft, Supervision.

## Declaration of competing interest

The authors declare that they have no known competing financial interests or personal relationships that could have appeared to influence the work reported in this paper.

## Acknowledgements

Sergio Santoro and Michele De Biase acknowledge the European Commission for the financial support activated under the PON "Research and Innovation" 2014–2020, Action I.2 "Researchers' Mobility", Notice D.D. 407 of 02.27.2018 - AIM "Attraction and International Mobility"-Line 2 "Researchers' Attraction" and Line 1 "Researcher's Mobility". The financial support of: the European Union through the project H2020-MSCA-RISE REMIND "Renewable Energies for Water Treatment and REuse in Mining Industries" (Grant agreement ID: 823948) is kindly acknowledged.

## References

[1] M. d'Halluin, J. Rull-Barrull, G. Bretel, C. Labrugère, E. Le Grognec, F.-X. Felpin, Chemically modified cellulose filter paper for heavy metal remediation in water, ACS Sustain. Chem. Eng. 5 (2017) 1965–1973, https://doi.org/10.1021/acssuschemeng.6b02768.

[2] S. Santoro, H. Estay, A.H. Avci, L. Pugliese, R. Ruby-Figueroa, A. Garcia, M. Aquino, S. Nasirov, S. Straface, E. Curcio, Membrane technology for a sustainable copper mining industry: the Chilean paradigm, Clean. Eng. Technol. 2 (2021), 100091, https://doi.org/10.1016/j.clet.2021.100091.

[3] R. Molinari, S. Gallo, P. Argurio, Metal ions removal from wastewater or washing water from contaminated soil by ultrafiltration–complexation, Water Res. 38 (2004) 593–600, https://doi.org/10.1016/j.watres.2003.10.024.

[4] IARC, Some drinking-water disinfectants and contaminants, including arsenic, in: IARC Monogr. Eval. Carcinog. Risks to Humans 84, 2004, pp. 1–477.

[5] P. Bhattacharya, A.H. Welch, K.G. Stollenwerk, M.J. McLaughlin, J. Bundschuh, G. Panaullah, Arsenic in the environment: biology and chemistry, Sci. Total Environ. 379 (2007) 109–120, https://doi.org/10.1016/j.scitotenv.2007.02.037.

[6] D.K. Nordstrom, Worldwide occurrences of arsenic in ground water, Science 296 (2002) 2143–2145, https://doi.org/10.1126/science.1072375.

[7] I. Herath, M. Vithanage, J. Bundschuh, J.P. Maity, P. Bhattacharya, Natural arsenic in global groundwaters: distribution and geochemical triggers for mobilization, Curr. Pollut. Rep. 2 (2016) 68–89, https://doi.org/10.1007/s40726-016-0028-2.

[8] K.A. Hudson-Edwards, J.M. Santini, Arsenic-microbe-mineral interactions in mining-affected environments, Minerals 3 (2013) 337–351, https://doi.org/10.3390/min3040337.

[9] P. Drahota, M. Filippi, Secondary arsenic minerals in the environment: a review, Environ. Int. 35 (2009) 1243–1255, https://doi.org/10.1016/j.envint.2009.07.004.

[10] J. Murray, M.R. Orué, E.de las M. López, V.H. García, A. Kirschbaum, Geological-geomorphological and geochemical control on low arsenic concentration in the Lerma valley groundwater between the two high arsenic geologic provinces of Chaco-Pampean plain and Puna, Sci. Total Environ. 699 (2020), 134253, https://doi.org/10.1016/j.scitotenv.2019.134253.

[11] J. Tapia, J. Murray, M. Ormachea, N. Tirado, D.K. Nordstrom, Origin, distribution, and geochemistry of arsenic in the Altiplano-Puna plateau of Argentina, Bolivia, Chile, and Perú, Sci. Total Environ. 678 (2019) 309–325, https://doi.org/10.1016/j.scitotenv.2019.04.084.

[12] J. Bundschuh, M.I. Litter, F. Parvez, G. Román-Ross, H.B. Nicolli, J.-S. Jean, C.-W. Liu, D. López, M.A. Armienta, L.R.G. Guilherme, A.G. Cuevas, L. Cornejo, L. Cumbal, R. Toujaguez, One century of arsenic exposure in Latin America: a review of history and occurrence from 14 countries, Sci. Total Environ. 429 (2012) 2–35, https://doi.org/10.1016/j.scitotenv.2011.06.024.

[13] S.J. Ravindran, S.K. Jenifer, J. Balasubramanyam, S.K. Jana, S. Krishnakumar, S. Elchuri, L. Philip, T. Pradeep, Arsenic toxicity: carbonate's counteraction revealed, ACS Sustain. Chem. Eng. 8 (2020) 5067–5075, https://doi.org/10.1021/acssuschemeng.9b06850.

[14] A. García-Sánchez, P. Alonso-Rojo, F. Santos-Francés, Distribution and mobility of arsenic in soils of a mining area (Western Spain), Sci. Total Environ. 408 (2010) 4194–4201, https://doi.org/10.1016/j.scitotenv.2010.05.032.
[15] F. Schwanck, J.C. Simões, M. Handley, P.A. Mayewski, R.T. Bernardo, F.E. Aquino, Anomalously high arsenic concentration in a West Antarctic ice core and its relationship to copper mining in Chile, Atmos. Environ. 125 (2016) 257–264, https://doi.org/10.1016/j.atmosenv.2015.11.027.
[16] R. Oyarzun, J. Lillo, P. Higueras, J. Oyarzún, H. Maturana, Strong arsenic enrichment in sediments from the Elqui watershed, Northern Chile: industrial (gold mining at El Indio-Tambo district) vs. geologic processes, J. Geochem.Explor. 84 (2004) 53–64, https://doi.org/10.1016/j.gexplo.2004.03.002.
[17] S. Bhowmick, B. Nath, D. Halder, A. Biswas, S. Majumder, P. Mondal, S. Chakraborty, J. Nriagu, P. Bhattacharya, M. Iglesias, G. Roman-Ross, D. G. Mazumder, J. Bundschuh, D. Chatterjee, Arsenic mobilization in the aquifers of three physiographic settings of West Bengal, India: understanding geogenic and anthropogenic influences, J. Hazard. Mater. 262 (2013) 915–923, https://doi.org/10.1016/j.jhazmat.2012.07.014.
[18] P.L. Smedley, D.G. Kinniburgh, in: O. Selinus (Ed.), Arsenic in Groundwater and the Environment BT - Essentials of Medical Geology: Revised Edition, Springer Netherlands, Dordrecht, 2013, pp. 279–310, https://doi.org/10.1007/978-94-007-4375-5_12.
[19] J.O. Nriagu, P. Bhattacharya, A.B. Mukherjee, J. Bundschuh, R. Zevenhoven, R. H. Loeppert, Arsenic in soil and groundwater: an overview, in: Arsen. Soil Groundw. Environ, Elsevier, 2007, pp. 3–60, https://doi.org/10.1016/S1875-1121(06)09001-8.
[20] M.A. Inam, R. Khan, M. Akram, S. Khan, D.R. Park, I.T. Yeom, Interaction of arsenic species with organic ligands: competitive removal from water by coagulation-flocculation-sedimentation (C/F/S), Molecules 24 (2019), https://doi.org/10.3390/molecules24081619.
[21] S. Mandal, M.K. Sahu, R.K. Patel, Adsorption studies of arsenic(III) removal from water by zirconium polyacrylamide hybrid material (ZrPACM-43), Water Resour. Ind. 4 (2013) 51–67, https://doi.org/10.1016/j.wri.2013.09.003.
[22] B. An, Z. Fu, Z. Xiong, D. Zhao, A.K. SenGupta, Synthesis and characterization of a new class of polymeric ligand exchangers for selective removal of arsenate from drinking water, React. Funct. Polym. 70 (2010) 497–507, https://doi.org/10.1016/j.reactfunctpolym.2010.01.006.
[23] M.C. Dodd, N.D. Vu, A. Ammann, V.C. Le, R. Kissner, H.V. Pham, T.H. Cao, M. Berg, U. von Gunten, Kinetics and mechanistic aspects of As(III) oxidation by aqueous chlorine, chloramines, and ozone: relevance to drinking water treatment, Environ. Sci. Technol. 40 (2006) 3285–3292, https://doi.org/10.1021/es0524999.
[24] J. Hou, J. Luo, S. Song, Y. Li, Q. Li, The remarkable effect of the coexisting arsenite and arsenate species ratios on arsenic removal by manganese oxide, Chem. Eng. J. 315 (2017) 159–166, https://doi.org/10.1016/j.cej.2016.12.115.
[25] P.V. Nidheesh, T.S.A. Singh, Arsenic removal by electrocoagulation process: recent trends and removal mechanism, Chemosphere 181 (2017) 418–432, https://doi.org/10.1016/j.chemosphere.2017.04.082.
[26] I. Ounifi, Y. Guesmi, C. Ursino, S. Santoro, S. Mahfoudhi, A. Figoli, E. Ferjanie, A. Hafiane, Antifouling membranes based on cellulose acetate (CA) blended with poly(acrylic acid) for heavy metal remediation, Appl. Sci. 11 (2021), https://doi.org/10.3390/app11104354.
[27] A. Figoli, C. Ursino, S. Santoro, I. Ounifi, J. Chekir, A. Hafiane, E. Ferjani, Cellulose acetate nanofiltration membranes for cadmium remediation, J. Membr. Sci. Res. 6 (2020) 226–234, https://doi.org/10.22079/jmsr.2020.120669.1336.
[28] A. Qayum, J. Wei, Q. Li, D. Chen, X. Jiao, Y. Xia, Efficient decontamination of multi-component wastewater by hydrophilic electrospun PAN/AgBr/Ag fibrous membrane, Chem. Eng. J. 361 (2019) 1255–1263, https://doi.org/10.1016/j.cej.2018.12.161.
[29] J. Yin, B. Deng, Polymer-matrix nanocomposite membranes for water treatment, J. Memb. Sci. 479 (2015) 256–275, https://doi.org/10.1016/j.memsci.2014.11.019.
[30] S. Santoro, I. Vidorreta, I. Coelhoso, J.C. Lima, G. Desiderio, G. Lombardo, E. Drioli, R. Mallada, J. Crespo, A. Criscuoli, A. Figoli, Experimental evaluation of the thermal polarization in direct contact membrane distillation using electrospun nanofiber membranes doped with molecular probes, Molecules 24 (2019) 638.
[31] S. Santoro, I.M. Vidorreta, V. Sebastian, A. Moro, I.M. Coelhoso, C.A.M. Portugal, J. C. Lima, G. Desiderio, G. Lombardo, E. Drioli, R. Mallada, J.G. Crespo, A. Criscuoli, A. Figoli, A non-invasive optical method for mapping temperature polarization in direct contact membrane distillation, J. Memb. Sci. 536 (2017) 156–166, https://doi.org/10.1016/j.memsci.2017.05.001.
[32] E. Curcio, X. Ji, G. Di Profio, A.O. Sulaiman, E. Fontananova, E. Drioli, Membrane distillation operated at high seawater concentration factors: role of the membrane on CaCO3 scaling in presence of humic acid, J. Membr. Sci. 346 (2010) 263–269, https://doi.org/10.1016/j.memsci.2009.09.044.
[33] L. Li, K.K. Sirkar, Influence of microporous membrane properties on the desalination performance in direct contact membrane distillation, J. Membr. Sci. 513 (2016) 280–293, https://doi.org/10.1016/j.memsci.2016.04.015.
[34] F. Macedonio, E. Drioli, Pressure-driven membrane operations and membrane distillation technology integration for water purification, Desalination 223 (2008) 396–409, https://doi.org/10.1016/j.desal.2007.01.200.
[35] S.N. McCartney, N.A. Williams, C. Boo, X. Chen, N.Y. Yip, Novel isothermal membrane distillation with acidic collector for selective and energy-efficient recovery of ammonia from urine, ACS Sustain. Chem. Eng. 8 (2020) 7324–7334, https://doi.org/10.1021/acssuschemeng.0c00643.
[36] T.M. Missimer, R.G. Maliva, Environmental issues in seawater reverse osmosis desalination: intakes and outfalls, Desalination 434 (2018) 198–215, https://doi.org/10.1016/j.desal.2017.07.012.
[37] A.H. Avci, S. Santoro, A. Politano, M. Propato, M. Micieli, M. Aquino, Z. Wenjuan, E. Curcio, Photothermal sweeping gas membrane distillation and reverse electrodialysis for light-to-heat-to-power conversion, Chem. Eng. Process. - Process Intensif. (2021), 108382, https://doi.org/10.1016/j.cep.2021.108382.
[38] M.M. Damtie, R.H. Hailemariam, Y.C. Woo, K.-D. Park, J.-S. Choi, Membrane-based technologies for zero liquid discharge and fluoride removal from industrial wastewater, Chemosphere 236 (2019), 124288, https://doi.org/10.1016/j.chemosphere.2019.07.019.
[39] T. Tong, M. Elimelech, The global rise of zero liquid discharge for wastewater management: drivers, technologies, and future directions, Environ. Sci. Technol. 50 (2016) 6846–6855, https://doi.org/10.1021/acs.est.6b01000.
[40] G. Zaragoza, J.A. Andrés-Mañas, A. Ruiz-Aguirre, Commercial scale membrane distillation for solar desalination, Npj Clean Water 1 (2018) 1–6, https://doi.org/10.1038/s41545-018-0020-z.
[41] A.K. Manna, M. Sen, A.R. Martin, P. Pal, Removal of arsenic from contaminated groundwater by solar-driven membrane distillation, Environ. Pollut. 158 (2010) 805–811, https://doi.org/10.1016/j.envpol.2009.10.002.
[42] P. Pal, A.K. Manna, Removal of arsenic from contaminated groundwater by solar-driven membrane distillation using three different commercial membranes, Water Res. 44 (2010) 5750–5760, https://doi.org/10.1016/j.watres.2010.05.031.
[43] B. Tomaszewska, J. Bundschuh, L. Pająk, M. Dendys, V.D. Quezada, M. Bodzek, M. A. Armienta, M.O. Muñoz, A. Kasztelewicz, Use of low-enthalpy and waste geothermal energy sources to solve arsenic problems in freshwater production in selected regions of Latin America using a process membrane distillation – research into model solutions, Sci. Total Environ. 714 (2020), 136853, https://doi.org/10.1016/j.scitotenv.2020.136853.
[44] R. Molinari, P. Argurio, Arsenic removal from water by coupling photocatalysis and complexation-ultrafiltration processes: a preliminary study, Water Res. 109 (2017) 327–336, https://doi.org/10.1016/j.watres.2016.11.054.
[45] R. Molinari, T. Poerio, P. Argurio, Selective separation of copper(II) and nickel(II) from aqueous media using the complexation–ultrafiltration process, Chemosphere 70 (2008) 341–348, https://doi.org/10.1016/j.chemosphere.2007.07.041.
[46] C.K. Jain, I. Ali, Arsenic: occurrence, toxicity and speciation techniques, Water Res. 34 (2000) 4304–4312, https://doi.org/10.1016/S0043-1354(00)00182-2.
[47] D. Lawless, N. Serpone, D. Meisel, Role of hydroxyl radicals and trapped holes in photocatalysis. A pulse radiolysis study, J. Phys. Chem. 95 (1991) 5166–5170, https://doi.org/10.1021/j100166a047.
[48] J. Ryu, W. Choi, Effects of TiO2 surface modifications on photocatalytic oxidation of arsenite: the role of superoxides, Environ. Sci. Technol. 38 (2004) 2928–2933, https://doi.org/10.1021/es034725p.
[49] P. Pookrod, K.J. Haller, J.F. Scamehorn, Removal of arsenic anions from water using polyelectrolyte-enhanced ultrafiltration, Sep. Sci. Technol. 39 (2005) 811–831, https://doi.org/10.1081/SS-120028448.
[50] S. Tangvijitsri, C. Saiwan, C. Soponvuttikul, J.F. Scamehorn, Polyelectrolyte-enhanced ultrafiltration of chromate, sulfate, and nitrate, Sep. Sci. Technol. 37 (2002) 993–1007, https://doi.org/10.1081/SS-120002250.
[51] A. Figoli, I. Fuoco, C. Apollaro, M. Chabane, R. Mancuso, B. Gabriele, R. De Rosa, G. Vespasiano, D. Barca, A. Criscuoli, Arsenic-contaminated groundwaters remediation by nanofiltration, Sep. Purif. Technol. 238 (2020), 116461, https://doi.org/10.1016/j.seppur.2019.116461.
[52] F. Scarciglia, A. Nicolaci, S. Del Bianco, T. Pelle, M. Soligo, P. Tuccimei, F. Marzaioli, I. Passariello, F. Iovino, Reforestation and soil recovery in a Mediterranean mountain environment: insights into historical geomorphic and vegetation dynamics in the Sila Massif,Calabria, southern Italy 194 (2020), 104707, https://doi.org/10.1016/j.catena.2020.104707.
[53] P.L. Smedley, D.G. Kinniburgh, A review of the source, behaviour and distribution of arsenic in natural waters, Appl. Geochem. 17 (2002) 517–568, https://doi.org/10.1016/S0883-2927(02)00018-5.
[54] H. Yang, W.-Y. Lin, K. Rajeshwar, Homogeneous and heterogeneous photocatalytic reactions involving As(III) and As(V) species in aqueous media, J. Photochem. Photobiol. A Chem. 123 (1999) 137–143, https://doi.org/10.1016/S1010-6030(99)00052-0.
[55] M. Bissen, M.-M. Vieillard-Baron, A.J. Schindelin, F.H. Frimmel, TiO2-catalyzed photooxidation of arsenite to arsenate in aqueous samples, Chemosphere 44 (2001) 751–757, https://doi.org/10.1016/S0045-6535(00)00489-6.
[56] S. Pirgalıoğlu, T.A. Özbelge, H.Ö. Özbelge, N. Bicak, Crosslinked polyDADMAC gels as highly selective and reusable arsenate binding materials, Chem. Eng. J. 262 (2015) 607–615, https://doi.org/10.1016/j.cej.2014.10.015.
[57] J. Sánchez, B.L. Rivas, S. Özgöz, S. Ötles, N. Kabay, M. Bryjak, Ultrafiltration assisted by water-soluble poly(diallyl dimethyl ammonium chloride) for As(V) removal, Polym. Bull. 73 (2016) 241–254, https://doi.org/10.1007/s00289-015-1483-4.
[58] S. Al-Obaidani, E. Curcio, F. Macedonio, G. Di Profio, H. Al-Hinai, E. Drioli, Potential of membrane distillation in seawater desalination: thermal efficiency, sensitivity study and cost estimation, J. Membr. Sci. 323 (2008) 85–98, https://doi.org/10.1016/j.memsci.2008.06.006.
[59] S. Santoro, R.A. Tufa, A.H. Avci, E. Fontananova, G. Di Profio, E. Curcio, Fouling propensity in reverse electrodialysis operated with hypersaline brine, Energy (2021), 120563, https://doi.org/10.1016/j.energy.2021.120563.
[60] D.M. Warsinger, J. Swaminathan, E. Guillen-Burrieza, H.A. Arafat, J.H. Lienhard V, Scaling and fouling in membrane distillation for desalination applications: a review, Desalination 356 (2015), https://doi.org/10.1016/j.desal.2014.06.031.
[61] T. Horseman, Y. Yin, K.S.S. Christie, Z. Wang, T. Tong, S. Lin, Wetting,Scaling, and Fouling in Membrane Distillation: State-of-the-Art Insights on Fundamental Mechanisms and Mitigation Strategies 1 (2021) 117–140, https://doi.org/10.1021/acsestengg.0c00025.

[62] M. Prisciandaro, V. Innocenzi, F. Tortora, G. di Celso, Reduction of fouling and scaling by calcium ions on an UF membrane surface for an enhanced water pre-treatment, Water 11 (2019), https://doi.org/10.3390/w11050984.
[63] W. Yu, D. Song, W. Chen, H. Yang, Antiscalants in RO membrane scaling control, Water Res. 183 (2020), 115985, https://doi.org/10.1016/j.watres.2020.115985.
[64] C.N. Sawyer, P.L. McCarty, G.F. Parkin, Chemistry for Environmental Engineering and Science, McGraw-Hill, New York, 2003.
[65] X. Guan, J. Du, X. Meng, Y. Sun, B. Sun, Q. Hu, Application of titanium dioxide in arsenic removal from water: a review, J. Hazard. Mater. 215–216 (2012) 1–16, https://doi.org/10.1016/j.jhazmat.2012.02.069.
[66] J. Cui, J. Du, S. Yu, C. Jing, T. Chan, Groundwater arsenic removal using granular TiO2: integrated laboratory and field study, Environ. Sci. Pollut. Res. 22 (2015) 8224–8234, https://doi.org/10.1007/s11356-014-3955-8.
[67] G. Solt, 19 - water and effluents, in: D.A. Snow (Ed.), Plant Eng. Ref. B, Second ed., Butterworth-Heinemann, Oxford, 2002, pp. 16–19, https://doi.org/10.1016/B978-075064452-5/50074-2.
[68] A. Ali, F. Macedonio, E. Drioli, S. Aljlil, O.A. Alharbi, Experimental and theoretical evaluation of temperature polarization phenomenon in direct contact membrane distillation, Chem. Eng. Res. Des. 91 (2013) 1966–1977, https://doi.org/10.1016/j.cherd.2013.06.030.
[69] A. Politano, G. Di Profio, E. Fontananova, V. Sanna, A. Cupolillo, E. Curcio, Overcoming temperature polarization in membrane distillation by thermoplasmonic effects activated by ag nanofillers in polymeric membranes, Desalination 451 (2019) 192–199, https://doi.org/10.1016/j.desal.2018.03.006.
[70] A. Alkhudhiri, N. Darwish, N. Hilal, Membrane distillation: a comprehensive review, Desalination 287 (2012) 2–18, https://doi.org/10.1016/j.desal.2011.08.027.
[71] J. Phattaranawik, R. Jiraratananon, A.G. Fane, Effect of pore size distribution and air flux on mass transport in direct contact membrane distillation, J. Membr. Sci. 215 (2003) 75–85, https://doi.org/10.1016/S0376-7388(02)00603-8.
[72] J. Phattaranawik, R. Jiraratananon, A.G. Fane, Heat transport and membrane distillation coefficients in direct contact membrane distillation, J. Membr. Sci. 212 (2003) 177–193, https://doi.org/10.1016/S0376-7388(02)00498-2.
[73] E. Curcio, E. Drioli, Membrane distillation and related operations—a review, Sep. Purif. Rev. 34 (2005) 35–86, https://doi.org/10.1081/SPM-200054951.
[74] J. Phattaranawik, R. Jiraratananon, Direct contact membrane distillation: effect of mass transfer on heat transfer, J. Membr. Sci. 188 (2001) 137–143, https://doi.org/10.1016/S0376-7388(01)00361-1.
[75] A. Lesimple, F.E. Ahmed, N. Hilal, Remineralization of desalinated water: methods and environmental impact, Desalination 496 (2020), 114692, https://doi.org/10.1016/j.desal.2020.114692.
[76] A.F. Mohammad, M.H. El-Naas, A.H. Al-Marzouqi, M.I. Suleiman, M., Al musharfy, optimization of magnesium recovery from reject brine for reuse in desalination post-treatment, J. Water Process Eng. 31 (2019), 100810, https://doi.org/10.1016/j.jwpe.2019.100810.
[77] B.L. Rivas, M.del C. Aguirre, E. Pereira, Retention properties of arsenate anions of water-soluble polymers by a liquid-phase polymer-based retention technique, J. Appl. Polym. Sci. 102 (2006) 2677–2684, https://doi.org/10.1002/app.24093.
[78] R. Molinari, T. Poerio, P. Argurio, Chemical and operational aspects in running the polymer assisted ultrafiltration for separation of copper(II)–citrate complexes from aqueous media, J. Membr. Sci. 295 (2007) 139–147, https://doi.org/10.1016/j.memsci.2007.03.002.
[79] L. Song, Permeate flux in crossflow ultrafiltration under intermediate pressures, J. Colloid Interface Sci. 214 (1999) 251–263, https://doi.org/10.1006/jcis.1999.6187.
[80] K. Gao, T. Li, J. Liu, B. Dong, H. Chu, Ultrafiltration membrane fouling performance by mixtures with micromolecular and macromolecular organics, Environ. Sci. Water Res. Technol. 5 (2019) 277–286, https://doi.org/10.1039/C8EW00642C.
[81] L. Ao, W. Liu, L. Zhao, X. Wang, Membrane fouling in ultrafiltration of natural water after pretreatment to different extents, J. Environ. Sci. 43 (2016) 234–243, https://doi.org/10.1016/j.jes.2015.09.008.
[82] S.K. Zaidi, A. Kumar, Experimental studies in the dead-end ultrafiltration of dextran: analysis of concentration polarization, Sep. Purif. Technol. 36 (2004) 115–130, https://doi.org/10.1016/S1383-5866(03)00207-7.
[83] L. Shi, J. Huang, L. Zhu, Y. Shi, K. Yi, X. Li, Role of concentration polarization in cross flow micellar enhanced ultrafiltration of cadmium with low surfactant concentration, Chemosphere 237 (2019), 124859, https://doi.org/10.1016/j.chemosphere.2019.124859.
[84] G. Howard, J. Bartram, Domestic Water Quantity, Service Level and Health, 2003.
[85] H.S. Usman, K. Touati, M.S. Rahaman, An economic evaluation of renewable energy-powered membrane distillation for desalination of brackish water, Renew. Energy 169 (2021) 1294–1304, https://doi.org/10.1016/j.renene.2021.01.087.
[86] M.B. Shakoor, I. Bibi, N.K. Niazi, M. Shahid, M.F. Nawaz, A. Farooqi, R. Naidu, M. M. Rahman, G. Murtaza, A. Lüttge, The evaluation of arsenic contamination potential, speciation and hydrogeochemical behaviour in aquifers of Punjab, Pakistan, Chemosphere 199 (2018) 737–746, https://doi.org/10.1016/j.chemosphere.2018.02.002.
[87] E. Shaji, M. Santosh, K.V. Sarath, P. Prakash, V. Deepchand, B.V. Divya, Arsenic contamination of groundwater: a global synopsis with focus on the Indian Peninsula, Geosci. Front. 12 (2021), 101079, https://doi.org/10.1016/j.gsf.2020.08.015.